CHALMERS

Dynamic Modelling of Heat Transfer Processes in a Supercritical Steam Power Plant

Master's Thesis in Sustainable Energy Systems

OLLE PALMQVIST

Department of Energy and Environment
Division of Energy Technology
Chalmers University of Technology
Göteborg, Sweden 2012
T2012-378

MASTER'S THESIS

Dynamic Modelling of Heat Transfer Processes in a Supercritical Steam Power Plant

Master's Thesis within the Sustainable Energy Systems Master's programme.

OLLE PALMQVIST

SUPERVISORS:
Robert Johansson
Tobias Wahlberg, Solvina
Veronica Olesen, Solvina

EXAMINER:
Klas Andersson

Department of Energy and Environment
Division of Energy Technology
Chalmers University of Technology
Göteborg, Sweden 2012

Dynamic Modelling of Heat Transfer Processes in a Supercritical Steam Power Plant
Master's Thesis within the Sustainable Energy Systems Master's programme
OLLE PALMQVIST

T2012-378
Department of Energy and Environment
Division of Energy Technology
Chalmers University of Technology
SE-412 80 Göteborg
Sweden
Telephone: +46 (0)31-772 1000

Chalmers Reproservice
Göteborg, Sweden, 2012

Dynamic Modelling of Heat Transfer Processes in a Supercritical Steam Power Plant

Master's Thesis within the Sustainable Energy Systems Master's programme

OLLE PALMQVIST
Department of Energy and Environment
Division of Energy Technology
Chalmers University of Technology

ABSTRACT

Flexible power plant control has considerable economical benefit for power plant owners in the liberalised and highly dynamic electricity market found in many countries. While offering a high degree of operational flexibility, sophisticated and highly automated power plant control schemes leads to less active interference on operation by power plant operators. Full-scope dynamic simulators offers an alternative environment where operators and engineers can develop crucial knowledge about plant dynamics. The focus in the present work is to develop a dynamic model of a supercritical steam power plant boiler that could serve as a representation of the boiler in a power plant simulator. The boiler model is separated into subcomponents; a water wall, two superheaters and an economizer. Each component consists of one discrete volume of flue gas respectively water that are able to exchange heat by radiation or convection. The dynamic 1-dimensional heat and mass balance equations are based on an ideally-stirred tank approximation. A fictional boiler were dimensioned, and simulations were carried out according to the sliding pressure operation principle where steam mass flow and pressure is varied directly proportional to the load. The simulation results indicate that water flow dynamic phenomena strongly govern the dynamic water temperature response during load changes.

Key words: Supercritical, once-through boiler, dynamic heat transfer, Dymola, Modelica, sliding pressure.

Acknowledgements

This thesis was carried out at Solvina, a technical consulting company in Göteborg, and I would like to extend my thanks to the people responsible for giving me this opportunity. I would also like to thank its employees for any help that they have given, especially Tobias Wahlberg and Veronica Olesen who have been supervising me and giving me much-needed advice.

I would also like to send my thanks to:

Robert Johansson, from Energy Technology at Chalmers, for supervising and providing me with helpful academic input.

Klas Andersson, my examiner, also from Energy Technology, for his assistance and guidance.

The Author, Göteborg 29/5–12

Nomenclature

Constants

σ	Stefan-Boltzmann constant	$[\mathrm{W/m^2\,K^4}]$

Dimensionless numbers

Nu	Nusselt number ($\mathrm{Nu} = \frac{h \cdot D}{k}$)	[—]
Pr	Prandtl number ($\mathrm{Pr} = \frac{\mathrm{Cp} \cdot \mu}{k}$)	[—]
Re	Reynolds number ($\mathrm{Re} = \frac{\dot{m} \cdot D}{\mu}$)	[—]

Greek symbols

ε	Emissivity	[—]
λ	Tube thickness	[m]
μ	Dynamic viscosity	[Pa s]
ρ	Density	$[\mathrm{kg/m^3}]$

Latin symbols

A	Area	$[\mathrm{m^2}]$
Cp	Specific heat capacity	[J/kg K]
D	Tube diameter	[m]
E	Exergy	[J/kg]
F	Specific Helmholtz free energy	[J/kg]
G	Specific Gibbs free energy	[J/kg]

g_{tot}	Total transport factor	$[\text{m}^2]$
H	Specific enthalpy	$[\text{J/kg}]$
h	Heat transfer coefficient	$[\text{W/m}^2\,\text{K}]$
k	Thermal conductivity	$[\text{W/m}\,\text{K}]$
L	Length	$[\text{m}]$
$\dot{m}$	Mass flow	$[\text{kg/s}]$
$\underline{\dot{m}}$	Mass flux	$[\text{kg/m}^2\,\text{s}]$
N	Number of tubes wide	$[—]$
p	Pressure	$[\text{Pa}]$
$\dot{Q}$	Heat flow	$[\text{W}]$
r	Tube radius	$[\text{m}]$
S	Specific entropy	$[\text{J/kg}\,\text{K}]$
S_T	Transverse pitch (tube spacing)	$[\text{m}]$
T	Temperature	$[\text{K}]$
ΔT_{lm}	Logarithmic mean temperature difference	$[\text{K}]$
t	Time	$[\text{s}]$
U	Overall heat transfer coefficient	$[\text{W/m}^2\,\text{K}]$
u	Specific internal energy	$[\text{J/kg}]$
V	Volume	$[\text{m}^3]$
V_F	View factor	$[—]$
X	Mass fraction	$[—]$

Subscripts

g	Gas
i	Inner
o	Outer
s	Solid

w	Water
wall	Furnace wall
z	Flue gas specie

Contents

1

Introduction

The liberalisation of the electricity market in many countries have introduced new challenges to power plant owners. With the extent of intermittent power sources such as wind and solar power steadily rising, there is considerable economic benefit for power plant owners to have flexible power plant control that allows the possibility to quickly cycle between different operating conditions. Plant operators interfere less actively on operation as plants are equipped with highly automated and sophisticated control schemes to meet this demand in flexibility.

Situations may arise where operators need to control the plant manually during faults or if the automated control is partially unavailable. To be able to quickly and correctly act to any of these events requires detailed knowledge of the mechanisms and behaviour of the plant, which is gained mainly by active interaction with the plant. As operators are interfering less with live operation, a simulator of the real process offers an alternative environment where operators can develop an understanding of plant dynamics.

Power plants operating at supercritical live steam conditions, above 221 bar and 374°C, have the benefit of relatively high thermal efficiencies and are commonly found in today's electricity market. Modern designs of supercritical power plants have operational flexibility and are highly automated, and thus there is a need for simulators of such plants.

Such a simulator requires dynamic models of the mass and heat transfer processes in the plant as well as a representation of the control scheme. Solvina, a technical consulting company in Göteborg, have developed plant operator simulators in Dymola for different kinds of power plants with subcritical steam cycles. The simulators include dynamic models of all the necessary components, e.g. furnace, turbine, valves, regulators and pumps. The present work is a continuation of Solvina's efforts with simulators, with the focus being to extend the existing

model toolbox to be valid also for supercritical steam cycles.

1.1 Aim and Objective

The purpose of the work is to develop dynamic models of the heat and mass transfer processes in a supercritical power plant boiler. Specifically it should be based on the characteristics of a coal fired supercritical power plant boiler. The model should be numerically robust and implemented in a flexible way to allow Solvina the possibility to couple it with existing in-house models to construct a simulator of a complete power plant.

The main objectives of the thesis are summarised below:

- Develop dynamic models for the heat and mass transfer processes in a supercritical boiler.
- Find some criteria to evaluate the boiler model dynamic behaviour.

1.2 Scope

A modern supercritical steam power plant has many components, e.g. a sophisticated control system, a series of pre-heating heat exchangers, steam turbines, pumps and other auxiliary equipment, and it is not in the scope of this thesis to include them all. The focus is to develop a general model that captures the most salient characteristics of a boiler of this type. This general model is thought to serve as a framework to be extended upon for specific use in a plant simulator. The main focus of the thesis is to formulate a mass and heat transfer model for a supercritical boiler and to implement it in Dymola. The main components to be included in the model are:

- The water wall, i.e. the tube section in the boiler firing zone.
- Economizer.
- Superheaters.

The combustion process is not considered, and it is assumed that complete combustion occurs with a known adiabatic combustion temperature.

The application of this model in a simulator requires that the equations are solvable at least in real time by a standard workstation computer, but the ability to speed up simulations faster than real time is preferable. Moreover, continuous integration is only available in time and thus the equations needs to be spatially discrete. These criteria directly excludes a number of modelling approaches, e.g. because of the latter a plug-flow model is not possible and because of the former a tank-in-series model with a large number of tanks is infeasible.

2

Theory

In this chapter, the theory of steam power plant technologies and their operating principles, as well as a description of the heat and mass transfer in their boilers, are given.

2.1 Steam Power Plant Technologies

Increasing the thermal efficiency is one of the key issues for an electric power generator. Apart from designing a steam power plant for minimised heat losses, the most obvious way of increasing the efficiency, according to the second law of thermodynamics, is by increasing the average temperature of heat added to the steam cycle. One way of achieving this is by increasing the live steam temperature.

Taking into account the thermodynamic properties of the working fluid, the steam, one finds that there is an optimum pressure for a given live steam temperature that maximises the work that is possible to extract in the turbine. The maximum possible useful work in the cycle is given by the exergy in the live steam state that enters the turbine, considering the heat rejection state in the condenser to be the ambient condition. The available energy, or the exergy, E between two end states is

$$E = \Delta H - T_0(\Delta S), \tag{2.1}$$

where ΔH is the enthalpy difference, ΔS the entropy difference, and T_0 the ambient condition for heat rejection. Figure 2.1 shows the available work for five different temperatures at varying pressure, where the condenser pressure is 0.031 bar and the heat rejection temperature 30°C. The conclusion is that the highest theoretical efficiency gain is achieved when increasing both the temperature and the pressure of the live steam.

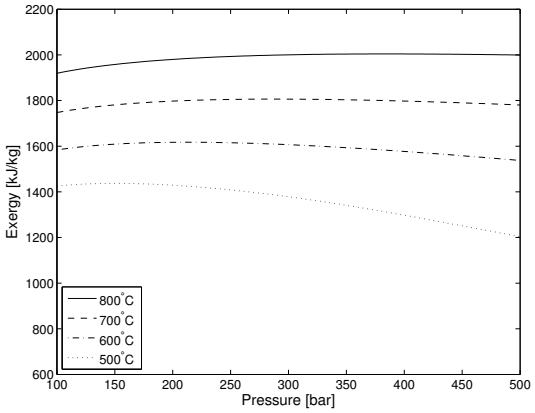

Figure 2.1: Available energy between the two end states of the steam cycle, from live steam to condenser state at different live steam conditions.

Choosing live steam conditions is more complicated when considering the complete steam cycle, including possible reheating stages and the preheating steam extractions in the turbine, but the general trend is to increase both the temperature and pressure for higher net efficiencies. In practice, the temperature and pressure is limited by the material in the boiler parts and the turbine. Owing to advances in material technology, state of the art steam power plants are today able to operate above the critical point, 221 bar and 374°C, at steam conditions above 600°C and 300 bar, having thermal efficiencies of around 45 % [1]. Research indicates that using nickel-alloys might allow even more extreme conditions, up to 700°C and 400 bar, making thermal efficiencies of 50 % or higher possible [2].

Many conventional subcritical boilers are equipped with a steam drum holding a large volume of water at equilibrium. Because of the density difference between the phases, the flow through the boiler can be upheld by natural circulation. Liquid water in the drum naturally falls down through the furnace, is heated and naturally rises up as vapour back to the drum.

Supercritical power plants differs from their subcritical counterpart in that it is not possible to distinguish a liquid and vapour phase when operating in the supercritical range, thus necessitating forced flow. Supercritical boilers are commonly called once-through boilers because the water passes only once through the boiler. The difference between the two boiler types is illustrated in Fig. 2.2(a) and Fig. 2.2(b).

Supercritical boilers are found either as a vertical construction where the gas flows vertically upwards throughout the boiler, or with two passes where the gas path changes direction, Fig. 2.2(c) illustrates a typical design of the latter.

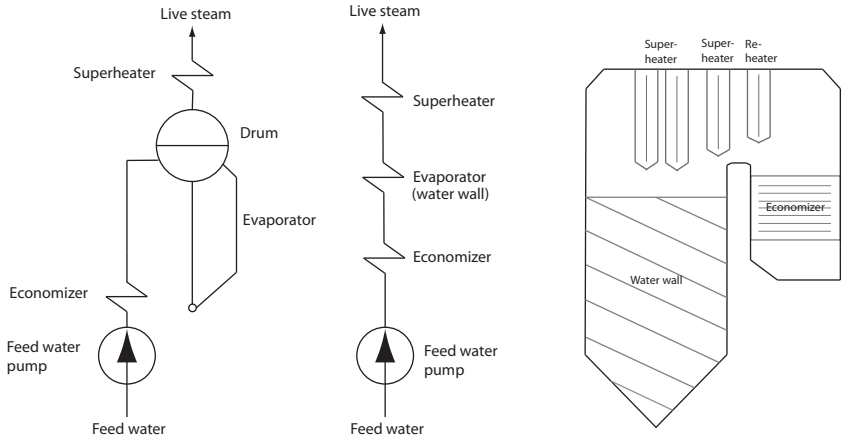

(a) Drum boiler. **(b)** Once-through boiler. **(c)** Two-pass once-through boiler design.

Figure 2.2: Two different types of boilers.

2.1.1 Heat Transfer in Supercritical Steam Power Plants

The steam cycles found in supercritical steam power plants are quite elaborate and includes a number of different heat transfer components. Apart from the boiler and its different heat transfer sections, a series of preheating heat exchangers are used to increase the average temperature of heat addition, and thus the efficiency. In the preheating heat exchangers, steam extracted at different pressure levels in the turbine is used to heat up the feed water.

In the boiler, which is the focus in the present work, convection and radiation are the dominating mechanisms of heat transfer, where the latter is usually responsible the majority of the total heat transfer in the furnace. Heat convection takes place both in the interior water flow, and in the exterior flue gas flow outside of the tubes. The interior heat transfer coefficient is usually several orders of magnitudes larger than the exterior heat transfer coefficient and can therefore usually be neglected [3].

As indicated by Fig. 2.2(b) and Fig. 2.2(c), the main heat transfer components in a supercritical boiler are the economizer, water wall and superheaters. Preheated water enters the boiler in the economizer where it is heated by the exiting flue gas. Because of the relatively low temperature of the flue gas, convection is the most important heat transfer mechanism in the economizer.

As the water leaves the economizer it is led to the water wall, which is a section of tubes in the high temperature firing zone of the furnace. The majority of the heat transfer in the boiler takes place in the water wall and radiation is the main mechanism. The tubes are either vertical or spiralling at an angle along the furnace

wall, the latter having an advantage that the water temperature profile is more uniform because local differences in heat flux are evened out as the fluid wraps around the furnace [2].

Finally the steam is superheated in two or more superheaters, situated at different locations in the furnace. Usually there is a primary superheater where water leaving the water wall is heated, mainly through convection. Before leaving the boiler the steam is heated in the radiant final superheater, which is situated in the boiler directly after the water wall in the flue gas flow path.

Reheating stages, where steam is heated to live steam temperature or slightly below after one or more of the high pressure turbine stages are also commonly found. They are used both as a measure to increase the thermal efficiency, and to allow expansion to lower pressures in the steam turbine while still avoiding damaging liquid droplet formation during the expansion.

Desuperheaters, or attemperators, are commonly found in steam boilers and acts as a fast control of the live steam temperature. If the temperature of the steam leaving the final superheater exceeds the target temperature, cooling water is injected through a valve that is controlled by a regulator.

2.1.2 Properties of Supercritical Water

Some substances have a critical point—such as the arbitrary fluid whose phase diagram is depicted in Fig. 2.3—at which a phase boundary ceases to exist. The critical point for water occurs at 220.6 bar and 374°C. The behaviour of fluids at near-critical condition is characterised by a strong dependence on temperature of their thermal and transport properties. In Fig. 2.4 this behaviour is illustrated for supercritical water, using the IAPWS-IF97 industry standard for calculation of the thermodynamic properties of state for water [4].

The rapid variation of thermal and transport properties in a region close to the critical point seen in Fig. 2.4 affects the internal heat transfer coefficient in the water wall. The effect can be seen as either an increase or decrease on the heat transfer coefficient and can locally be very strong, an example of which is the that the heat capacity increases by a factor 10 at 250 bar, Fig. 2.4(a) [5].

In a subcritical boiler, the heat transfer coefficient in the boiling region will strongly influence the total heat transfer because of the significant boiling enthalpy. The transition to supercritical state is in some regards analogous to boiling, i.e. the viscosity and density changes from liquid-like to vapour-like, but there is no analogue to the boiling enthalpy. The effect on the heat transfer coefficient may be strong locally, but because it occurs only in a narrow temperature range the enthalpy rise is small, and thus the effect on the total heat transfer is limited [5].

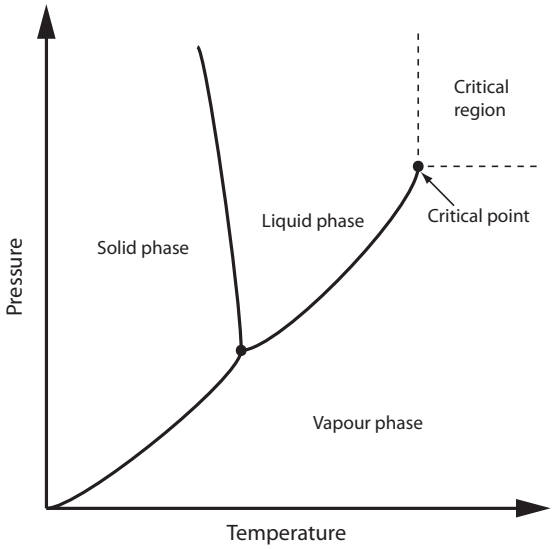

Figure 2.3: A general phase diagram.

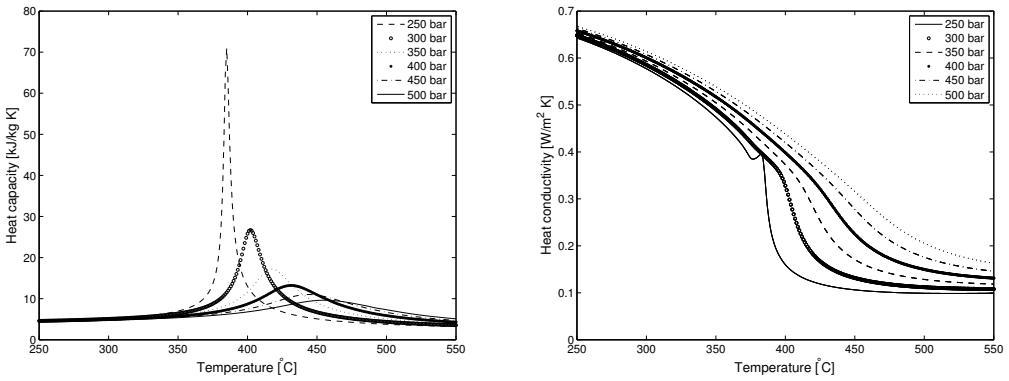

(a) Specific heat capacity as a function of temperature.

(b) Thermal conductivity as a function of temperature.

Figure 2.4: Thermal property variability at near-critical conditions.

2.2 Operation of Once-Through Boilers

Frequent load cycling has implications on the design and operation of the plants, and thermal stress is one of the limiting factors as to what load changes the plant can sustain. Thermal stress arises in the turbine and boiler parts due to local temperature changes, and may in the long run lead to mechanical failure.

The nature of a turbine is to require less pressure as the steam flow is reduced with the load, and thus the pressure at the turbine inlet needs to be controlled to

keep the rotating speed constant. Depending on how this is handled, power plants with load changing capability are grouped into two categories, constant pressure and sliding pressure.

Constant pressure operation is commonly found in subcritical steam power plants where the boiler supplies a constant outlet pressure which is then reduced through admission valves to the pressure required by the turbine. Pressure throttling leads to efficiency losses, which can be significant at low load operation. Moreover, thermal stress in the turbine blades can arise because of variations in the inlet steam temperature when throttling the flow, according to the Joule-Thomson effect [6].

Once-through boilers lend themselves well to sliding pressure operation where instead the live steam pressure is directly proportional to the load demand in the steam turbine. The main advantage of this operating principle is that the turbine admission valves can be left fully opened. The reduced throttling losses, and the reduced work required by the feed pumps allows the unit to operate at higher efficiencies over a wide load range [2].

Realising the sliding pressure principle in actual operation requires a highly advanced control system. Supercritical power plants employ coordinated control of the complete steam cycle, including e.g. feed water pressure and flow, fuel and firing system, turbine and preheating heat exchangers. These systems needs to be able to handle rapidly changing operational conditions, and the technically advanced solutions impose a high capital cost [2].

Figure 2.5 shows a pressure-enthalpy diagram for an idealised boiler steam cycle with no pressure losses in a pure sliding pressure supercritical power plant rated at 300 bar and 600°C at different loads. The definition of the load stems from the steam turbine which at a certain time requires a certain pressure and steam flow rate. The water mass flow rate and pressure are thus both directly proportional to the load, as it is defined here. Thus, a load change will henceforth refer to a change in mass flow and pressure of water.

The control system in a supercritical power plant is, as mentioned, quite complex, but the principle is that the steam turbine determines the load i.e. feed water flow and pressure. The firing rate in the boiler is then adjusted accordingly so that the live steam temperature is maintained at the target level which in this example is 600°C [2]. Keeping the temperature at a constant level is preferable as it limits the thermal stress. The lag-times in a boiler are considerable, and therefore some kind of model predictive feedforward logic is employed for the firing control, and in effect the firing rate can be adjusted at the same time as the feed water pressure and flow is changed [2].

As the boiler reaches low loads, it is slightly more efficient with a lower live steam temperature [2]. This is illustrated in Fig. 2.5 at 60 % load as a slight temperature decrease.

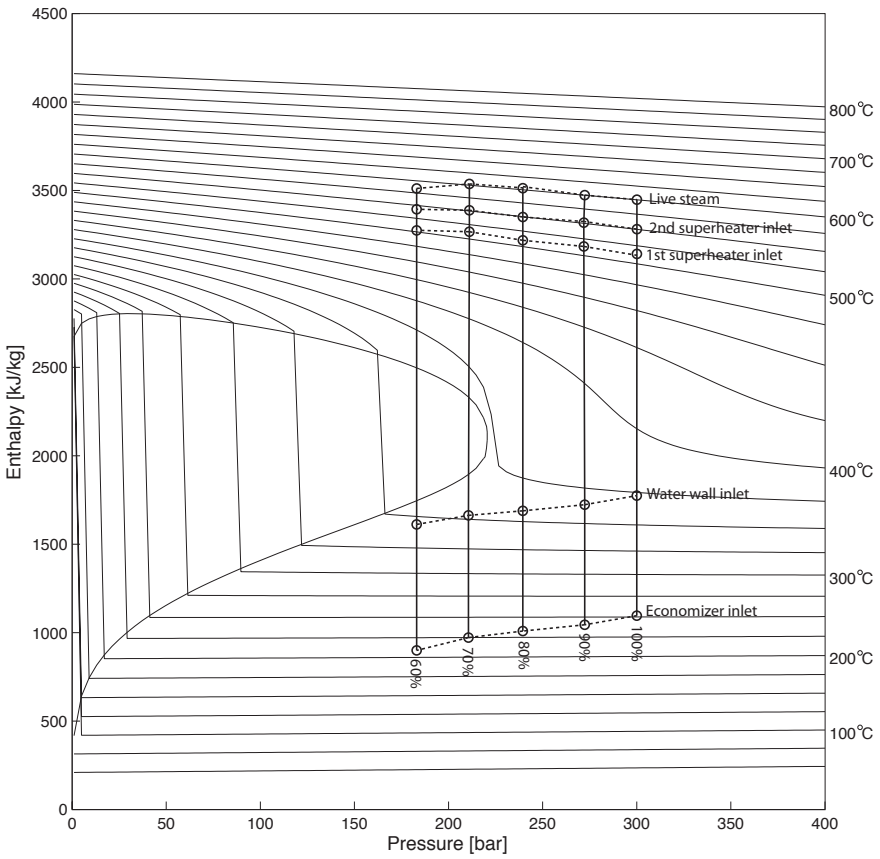

Figure 2.5: Enthalpy-pressure diagram showing the enthalpy and temperature rise in the boiler components at different loads [2].

Since supercritical boilers have no steam drum, and thus little thermal inertia, they can sustain rapid ramp-up and ramp-down rates in power output. Load transients of 4-6 % of maximum rated power output per minute are possible over a wide output power range [7].

Because two-phase flow occurs in part of the load range of a sliding pressure boiler, special considerations for the design of the boiler are required. It is crucial that the steam mass flow is enough to cool the water wall tubes to avoid material failure. One of the effects of designing for appropriate cooling at low load operation is a small flow area, which implicates a very high pressure drop, commonly around 30 to 40 bar, during full load operation [8].

Two-phase flow also has implications on the operation of the plant, mainly affecting the startup procedure. During cold startups, the main steam valve is closed and a recirculation pump is used to circulate the water until the furnace is hot enough for live operation. The water wall cannot produce completely dry

steam under these circumstances and because it is important to avoid introducing liquid water in the superheaters, a separator, commonly a Sulzer bottle, is installed to separate liquid water from dry steam. The liquid water is directly led back to the water wall, and separate streams of the dry steam is routed through the superheaters and reheaters before it is led back to the water wall. When the target temperatures are met, live operation starts and the separator is bypassed [2].

2.3 Heat Transfer

Throughout the furnace, water flows in tubes with different geometries and arrangements and exchanges heat with the external flue gas flow through radiation, convection and conduction. A schematic illustration of the heat transfer in any heat exchange component in the furnace can be seen in Fig. 2.6. Even though Fig. 2.6 indicates countercurrent flow, both crossflow and concurrent flow also occurs in the furnace.

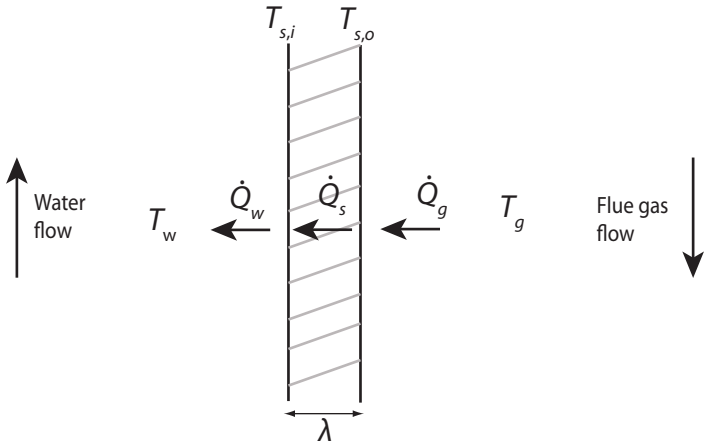

Figure 2.6: Schematic illustration of the heat transfer. $\dot{Q}_g$ is both convective and radiative heat transfer, $\dot{Q}_g$ is conduction through the tubes, and $\dot{Q}_w$ is convective heat transfer.

Equations (2.2) through (2.6) describe the heat transferred between flue gas and tube, and between tube and water.

$$\dot{Q}_{\mathrm{g}} = \dot{Q}_{\mathrm{g,rad}} + \dot{Q}_{\mathrm{g,conv}} \tag{2.2}$$

$$\dot{Q}_{\mathrm{g,rad}} = A_o \varepsilon \sigma (T_g^4 - T_{s,o}^4) \tag{2.3}$$

$$\dot{Q}_{\mathrm{g,conv}} = A_o h_g (T_g - T_{s,o}) \tag{2.4}$$

$$\dot{Q}_{\mathrm{s}} = k\lambda (T_{s,o} - T_{s,i}) \tag{2.5}$$

$$\dot{Q}_{\mathrm{w}} = A_i h_w (T_{s,i} - T_w) \tag{2.6}$$

At steady state, the heat flows are equal,

$$\dot{Q}_g = \dot{Q}_s = \dot{Q}_w. \tag{2.7}$$

The external heat transfer coefficient, h_g, is usually in the order of $100\,\mathrm{W/m^2\,K}$, while the internal heat transfer coefficient, h_w, is around $1\,000 - 20\,000\,\mathrm{W/m^2\,K}$, depending on the phase [3]. As mentioned in Chapter 2.1.1, heat transfer due to internal convection (Eq. (2.6)) is therefore negligible.

Heat transfer resistance due to conduction is also negligible considering the high conductivity and the thickness of the tube material. However, the combined tonnage of all the tubes is considerable in a typical boiler, and the thermal inertia of all that mass has an effect on the dynamic behaviour of the boiler. Obviously, heating up the tubes during a cold startup takes a considerable amount of time, but the effect is less important during live operation. Because startups are not considered in, the thermal inertia effect is neglected.

The heat transfer equations that are left when neglecting conduction and internal convection are

$$\dot{Q}_\mathrm{g} = \dot{Q}_\mathrm{g,rad} + \dot{Q}_\mathrm{g,conv}, \tag{2.8}$$

$$\dot{Q}_\mathrm{g,rad} = A_o \varepsilon \sigma (T_g^4 - T_w^4), \tag{2.9}$$

$$\dot{Q}_\mathrm{g,conv} = A_o h_g (T_g - T_w). \tag{2.10}$$

Empirical correlations used for the convective heat transfer coefficient (h) as well as expressions for the emissivity (ε) are described in the following paragraphs.

2.3.1 Radiation

Radiation in the furnace chamber is a complex phenomenon that depends on e.g. the flue gas temperature and composition, particulate flow, furnace geometry, tube material, and the flame properties. The above expression (Eq. (2.9)) is a simplification of the radiation heat transfer that is based on a number of assumptions. Most important is a tank reactor-assumption, meaning that the flue gas temperature is assumed to be uniform in the combustion chamber and that the heat flux is uniformly distributed.

The point of origin is the radiation equation

$$\dot{Q}_{g,\mathrm{rad}} = g_\mathrm{tot} \sigma (T_g^4 - T_{s,o}^4), \tag{2.11}$$

where g_tot is the total transport factor. Radiation is exchanged between the gas and the tube surface, between the gas and furnace wall, and between the furnace wall and tube surface. Assuming the gas emissivity is equal for radiation exchange between all surfaces, an expression for g_tot can be found as

$$g_\mathrm{tot} = \frac{1}{\dfrac{1-\varepsilon_s}{A_s \varepsilon_s} + \dfrac{1}{\varepsilon_g}\left(A_s + \dfrac{A_g}{1 + \varepsilon_g/(1-\varepsilon_g) V_F}\right)^{-1}}, \tag{2.12}$$

where V_F is the view factor from a non-cooled furnace wall to the tubes,

$$V_F = \frac{A_s}{A_s + A_{\text{wall}}}. \tag{2.13}$$

For a furnace wall that is completely covered with tubes, Eq. (2.12) simplifies to

$$g_{\text{tot}} = \frac{A_s}{\frac{1}{\varepsilon_s} + \frac{1}{\varepsilon_g} - 1}. \tag{2.14}$$

This simplified form of the total transport factor is conveniently expressed as the product of A_s and the total effective emissivity ε, i.e.

$$g_{\text{tot}} = A_s \varepsilon, \tag{2.15}$$

where

$$\varepsilon = \left(\frac{1}{\varepsilon_s} + \frac{1}{\varepsilon_g} - 1 \right)^{-1}, \tag{2.16}$$

letting $A_s = A_o$ gives

$$\dot{Q}_{\text{g,rad}} = A_o \varepsilon \sigma (T_g^4 - T_{s,o}^4), \tag{2.17}$$

and since conduction is neglected, Eq. (2.9) for the heat flow is finally obtained

$$\dot{Q}_{\text{g,rad}} = A_o \varepsilon \sigma (T_g^4 - T_w^4).$$

Tabulated values for the emissivity of different types of tube materials are readily available. The emissivity for the the gas however is more complicated as it varies with composition, temperature and pressure. The main radiating species in the flue gas are CO_2, H_2O and entrained solid particles. The radiation spectrum of these species overlap to some extent, leading to interference. A commonly employed method for calculation of the combined emissivity of CO_2 and H_2O, at partial pressures commonly found in flue gas, is the weighted sum of grey gases model [9]. The combined total emission coefficient can then be calculated by Eq. (2.16) since both ε_s and ε_g are known.

A more simplified approach to finding the total effective emissivity is to use empirical data for the combined influence of flue gas, particles and the furnace wall on the emission coefficient. In Tab. 2.1 such data is presented for a number of different common fuel types [10].

Table 2.1: Typical total effective emissivities for a few different types of fuels

Fuel type	ε
Bituminous coal	0.30-0.45
Lignite	0.40-0.55
Oil	0.45-0.60
Natural gas	0.55-0.70

2.3.2 External Convection

Convective heat transfer components in a boiler are usually found as tube banks. The tubes are usually either bare or they have area-increasing fins, the latter is common in the economizer. The arrangement is either staggered or in-line, the difference is illustrated in Fig. 2.7.

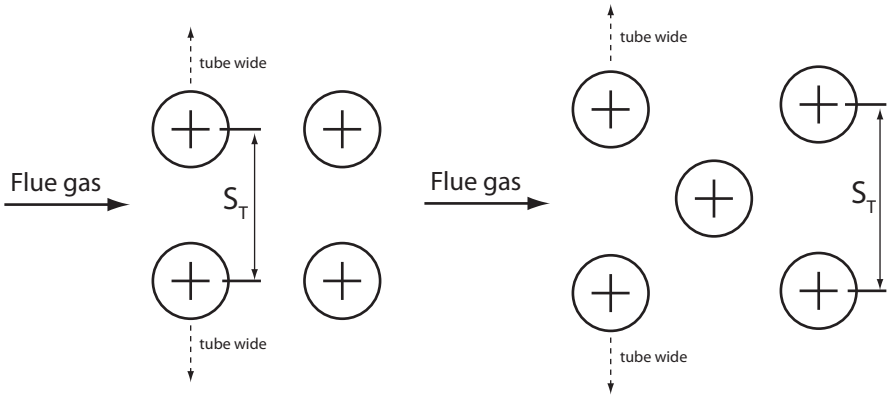

Figure 2.7: In-line (left) and staggered (right) tube bank arrangement.

The most common approach to finding heat transfer coefficients is by means of empirical dimensionless relations. There exist many different correlations depending on the flow condition as well as the arrangement of tubes and whether they are finned or not. Finned tube correlations are more complex and have more parameters, and sometimes the tube manufacturer supply correlations specific to their tube designs. Because no specific tube bank design is considered in the present work, a simple bare tube correlation is used. While a bare tube correlation likely gives a conservative estimate of the external heat transfer coefficient, it does capture the important flow depending dynamics. One such correlation for in-line and staggered arrangement is given by Eq. (2.18) [11, 12].

$$\mathrm{Nu} = 0.33\,\mathrm{Re}^{0.6}\mathrm{Pr}^{0.33}. \tag{2.18}$$

The heat transfer coefficient in turn is given by the Nusselt number,

$$\mathrm{Nu} = \frac{h_g D}{k_g}. \tag{2.19}$$

The Reynolds number is given by

$$\mathrm{Re} = \frac{\underline{\dot{m}}_g D}{\mu}, \tag{2.20}$$

the Prandtl number by

$$\mathrm{Pr} = \frac{\mathrm{Cp}\mu}{k}, \tag{2.21}$$

and the gas mass flux $\underline{\dot{m}}_g$ by

$$\underline{\dot{m}}_g = \frac{\dot{m}_g}{NL(S_T - D)}. \tag{2.22}$$

2.3.3 Heat Exchanger Model

A common approach to modelling the heat transfer in a countercurrent heat exchanger where convection is the governing heat transfer mechanism is by

$$\dot{Q} = AU\Delta T_{\mathrm{lm}}, \tag{2.23}$$

where U is the overall heat transfer coefficient. The logarithmic mean temperature difference, where ΔT_1 and ΔT_2 are the temperature differences at the two ends of the heat exchanger, is defined as

$$\Delta T_{\mathrm{lm}} = \frac{\Delta T_1 - \Delta T_2}{\ln \dfrac{\Delta T_1}{\Delta T_2}}. \tag{2.24}$$

The overall heat transfer coefficient for heat transfer through a tube with inner radius r_i and outer radius r_o, based on the exterior area, is given by Eq. (2.25) [13].

$$U = \left(\frac{A_o}{A_i h_w} + \frac{A_o \ln(r_o/r_i)}{2\pi k \lambda} + \frac{1}{h_g} \right)^{-1}. \tag{2.25}$$

As both conduction and the internal convection is neglected, Eq. (2.25) simplifies to

$$U = h_g. \tag{2.26}$$

3

Model Structure

The model is separated into a number of different modules corresponding to the physical components discussed before. Included in the model are the water wall, two superheaters and an economizer. Figure 3.1 shows the flow paths and how the components are connected to each other.

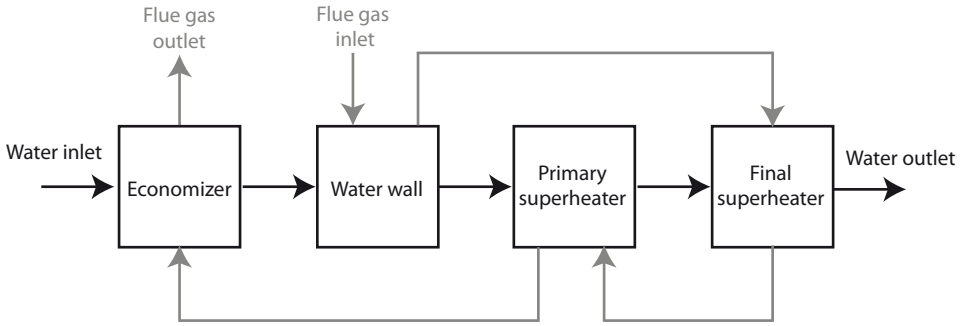

Figure 3.1: Water (black) and flue gas (grey) flow paths through the model components.

Each model component is composed of a number of subcomponents; one 1-dimensional flow component for flue gas respectively water and a heat transfer interface. The principle of a flow component is illustrated by Fig. 3.2. This modular design approach makes it possible to reuse subcomponents, e.g. the flow models are common to all the components. A flow component can also act as an adiabatic tank by not connecting it to a heat transfer interface.

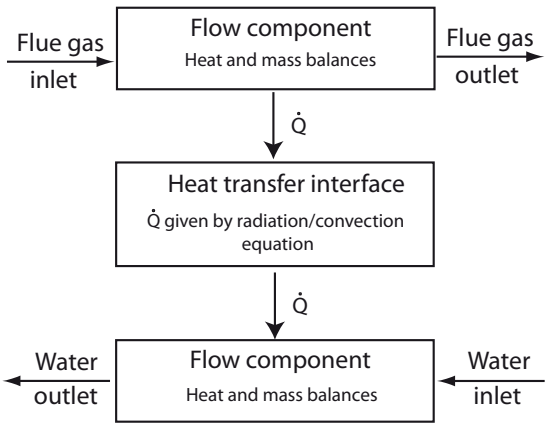

Figure 3.2: Outline of a heat exchanging component.

3.1 Mass and Heat Balances

The flow component includes the balance equations, and is in principle an ideally-stirred tank model, meaning that the water and flue gas states in one volume are evaluated at the outlet. The dynamic 1-dimensional mass and heat balances in the flow components are given by Eq. (3.1) and (3.2).

$$\frac{\mathrm{d}}{\mathrm{d}t}\left(V \cdot \rho_{\mathrm{out}} \cdot u_{\mathrm{out}}\right) = \dot{Q} + \dot{m}_{\mathrm{in}} H_{\mathrm{in}} - \dot{m}_{\mathrm{out}} H_{\mathrm{out}}, \tag{3.1}$$

$$\frac{\mathrm{d}}{\mathrm{d}t}\left(V \cdot \rho_{\mathrm{out}}\right) = \dot{m}_{\mathrm{in}} - \dot{m}_{\mathrm{out}}. \tag{3.2}$$

There is one mass balance for every specie z with mass fraction X_z in the flue gas,

$$\frac{\mathrm{d}}{\mathrm{d}t}\left(V \cdot \rho_{\mathrm{out}} \cdot X_{z,\mathrm{out}}\right) = \dot{m}_{z,\mathrm{in}} - \dot{m}_{z,\mathrm{out}}, \tag{3.3}$$

and the sum of mass fractions equal 1,

$$\sum X_z = 1. \tag{3.4}$$

However, it is assumed that the flue gas composition remains unchanged,

$$X_{z,\mathrm{in}} = X_{z,\mathrm{out}}, \tag{3.5}$$

and thus Eq. (3.3) is replaced by a single mass balance

$$\frac{\mathrm{d}}{\mathrm{d}t}\left(V \cdot \rho_{\mathrm{out}}\right) = \sum \dot{m}_{z,\mathrm{in}} - \sum \dot{m}_{z,\mathrm{out}}. \tag{3.6}$$

The main species in the flue gas of a coal fired power plant are N_2, CO_2, H_2O and O_2. Other species occur only in trace amounts do not greatly influence the heat transfer. Solvina have developed a eight-specie mixture model that includes four more species apart from the above. Because all the model components developed needs to be compatible with existing in-house models at Solvina, this eight-specie mixture model is used.

The ideally-stirred tank approximation has an impact on the accuracy of the model. For the water flow where no mixing occurs in the flow direction, a more accurate representation could be to use mean values of the inlet and outlet state properties, i.e. replacing the accumulation term in the heat balance with

$$\frac{\mathrm{d}}{\mathrm{d}t}\left(V\left[\frac{\rho_{\mathrm{in}}+\rho_{\mathrm{out}}}{2}\right]\left[\frac{u_{\mathrm{in}}+u_{\mathrm{out}}}{2}\right]\right)$$

and similarly in the mass balance. The same is true for the flue gas, but the extent is likely less because some degree of mixing does occur. Because using mean values in the accumulation term adds significantly to the numerical complexity of the problem, it was not considered.

The pressure loss is not modelled in the components, but it can be included on the water side as a parameter Δp_{loss}, i.e.

$$p_{\mathrm{out}} = p_{\mathrm{in}} - \Delta p_{\mathrm{loss}}. \tag{3.7}$$

3.2 Heat Transfer Interface

The heat transfer interface specifies equations for the heat flow $\dot{Q}$ in the heat balance (Eq. (3.1)). Heat conduction is not included in the model, for reasons discussed in Chapter 2.3, and heat losses through the boiler walls are not considered.

Disregarding conduction, two different heat transfer interfaces are defined; one for radiative heat transfer and one for convective heat transfer. Radiation is the governing heat transfer mechanism in the water wall and final superheater, and convection is thus neglected. Radiation heat transfer is less important in the economizer and primary superheater, and only external convection is modelled in these components.

While the balance equations are based on an ideally-stirred tank approximation, representative mean values of the inlet and outlet temperatures are used to calculate the total heat transfer in a component. However, the thermal and transport properties used in the expressions for Reynolds and Prandtl numbers are calculated from the medium outlet states of a component. The rationale for not using mean values is the same as discussed in Chapter 3.1 regarding the accumulation term.

3.2.1 Water Wall and Final Superheater

Only radiation is considered for the water wall and final superheater components, and the heat flow is determined by Eq. (2.9),

$$\dot{Q} = A\varepsilon(T_g^4 - T_w^4).$$

The effective emissivity as well as the heat transfer area are parameters given as inputs by the model user. The representative temperatures T_g and T_w in the radiation equation are given by the arithmetic mean temperatures of flue gases respectively water

$$T_{\text{mean}} = \frac{T_{\text{in}} + T_{\text{out}}}{2}. \tag{3.8}$$

3.2.2 Primary Superheater and Economizer

The primary superheater and the economizer resembles countercurrent heat exchangers, and the heat transfer is therefore calculated using Eq. (2.23),

$$\dot{Q} = AU\Delta T_{\text{lm}}.$$

The overall heat transfer coefficient U is determined by the external heat transfer coefficient given by Eq. (2.18). The tube arrangement and tube dimensions, used in the convective heat transfer correlation, and the total available heat transfer area, A, are then parameters to the model.

The logarithmic mean temperature (Eq. (2.24)) is unsuitable for direct usage in dynamic simulations because of its numerical properties when $\Delta T_1 \simeq \Delta T_2$ and $\Delta T_1 \cdot \Delta T_2 = 0$. Therefore, a conditional expression is used so that when $|\Delta T_1 - \Delta T_2| < 0.05 \max(|\Delta T_1|, |\Delta T_2|)$

$$\Delta T_{\text{lm}} = 0.5\,(\Delta T_1 + \Delta T_2)\left[1 - \frac{1}{12}\frac{(\Delta T_1 - \Delta T_2)^2}{\Delta T_1 \Delta T_2}\left(1 - \frac{1}{2}\frac{(\Delta T_1 - \Delta T_2)^2}{\Delta T_1 \Delta T_2}\right)\right] \tag{3.9}$$

and when $\Delta T_1 \cdot \Delta T_2 = 0$ the arithmetic mean, Eq. (3.10), is used to avoid division with zero [14].

$$\Delta T_{\text{lm}} = 0.5\,(\Delta T_1 + \Delta T_2)\,. \tag{3.10}$$

3.2.3 Summary of Heat Transfer Equations

Table 3.1 summarises the equations that are used for the heat transfer in the different components.

Table 3.1: Summary of heat transfer equations

	Heat transfer mechanism	**Equations**
Water wall	Radiation	Eq. (2.9)
Primary superheater	Convection	Eq. (2.18) and (2.23)
Final superheater	Radiation	Eq. (2.9)
Economizer	Convection	Eq. (2.18) and (2.23)

3.3 Desuperheater

Included in the model is also a desuperheater, the control logic of which is shown in Fig. 3.3. Cooling water is injected in the valve and equilibrates with the steam in an adiabatic tank, i.e. a water flow component, and the temperature leaving the tank is the feedback signal to the regulator. Both the regulator and the control valve model have been developed by Solvina.

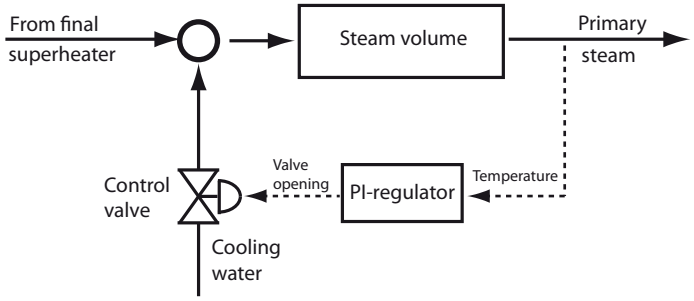

Figure 3.3: A schematic illustration of the desuperheater logic.

3.4 Water and Flue Gas Media

The water and flue gas media models used in the present work are both obtained from previous work, and some details on them are given the following paragraphs.

3.4.1 Water

Thermodynamic and transport properties for water are defined by the IAPWS-IF97 standard, which is commonly found in process engineering modelling tools. The water state is determined by the thermodynamic potentials Gibbs free energy or Helmholtz free energy, depending on the water phase. Fundamental equations for the thermodynamic potentials are defined, with the state variables temperature and pressure for Gibbs energy, and temperature and density for Helmholtz [4].

All other state properties, such as entropy, heat capacity and enthalpy, are attained as functions in terms of the Gibbs (G) or Helmholtz (F) energy and their state variable derivatives, i.e.

$$H(T,p) = G(T,p) - T\left(\frac{\partial G(T,p)}{\partial T}\right)_p \tag{3.11}$$

or

$$H(T,\rho) = F(T,\rho) - T\left(\frac{\partial F(T,\rho)}{\partial T}\right)_\rho + \rho\left(\frac{\partial F(T,\rho)}{\partial \rho}\right)_T. \tag{3.12}$$

"Backward" equations that are numerically consistent with the basic equations for Helmholtz and Gibbs free energy, are also defined in forms of $T(p,h)$ and $T(p,s)$, which makes it possible to calculate properties in in a combination of different ways, e.g. $h(p,s)$ via the relation $h(p,T(p,s))$. This makes computation of the commonly used properties highly efficient, and is the reason why the IAPWS-IF97 formulation is suitable for use in dynamic simulations [4].

Also included in the IAPWS formulation are transport properties such as kinematic viscosity and thermal conductivity.

3.4.2 Flue Gas

The flue gas media model used in this work has been developed by Solvina, and is an ideal gas mixture model of eight species; O_2, H_2O, N_2, CO, CO_2, H_2SO_4, SO_2 and NO. The model also handles condensation of water. The gas mixture state is characterised by three state variables; two thermal properties as well as some characteristic of the mixture, e.g. mass fraction. Transport properties such as the viscosity and conductivity are approximated by those of air at the same temperature and pressure.

3.5 Solution Method

The modelling environment used in the present work is Dymola which is a commercial modelling and simulation tool for dynamic systems based on Modelica and is one of the tools used at Solvina. Over the years, Solvina have developed an extensive in-house Modelica library of components and interfaces specific for their applications. Relevant to modelling of a power plant are e.g. models of turbines, pumps, valves, tanks, pipes, fittings and flue gas media.

The Modelica Standard Library is an open-source library, also developed by the Modelica Association, that provides a number of model components, interfaces and numerical functions. It includes a library of media models describing the thermodynamic and transport properties of many liquid and gas media, among

them the IAPWS-IF97 thermodynamic property formulation of water which is used in the present work.

3.5.1 Modelica

There are two distinctly different approaches to dynamic process modelling programs, either sequential modular or equation based. In a sequential environment, the model creator develops models for each of the components of the process. The inputs and outputs, in effect the flow directions, of each module are pre-defined by the developer, and solutions to the system are obtained by sequential execution of the modules according to some pre-defined order.

The sequential modular approach is common in many thermodynamical process modelling tools where the flow direction is usually known. To illustrate the solution process, consider two reactors coupled in series. All the variables are initialised, then a time step is taken and the equations are solved for the first reactor. The outputs of the first reactor in the previous time step, e.g. enthalpy, mixture variables and mass flow, are then used as inputs to the second reactor. The outputs of the second reactor is now calculated, and so forth. The model creator needs to be deeply involved in developing a method for solving the system, but the result can be very robust models.

Modelica is an example of the latter approach, the equation based, and is a modelling language specifically developed for dynamic modelling of large and complex physical systems. In Modelica, the governing equations are expressed in a declarative form, the compiler then manipulates the equations and arrives at a set of equations that are solved simultaneously by some solver. Modelling languages based on this approach are also said to be acausal, in the sense that there is no pre-defined direction of data flow [15].

An example of an acausal system is an electrical resistor where it cannot be determined whether it is the current that causes voltage, or vice versa. In a causal modelling environment, such a system needs to be translated into a set of computable equations that are evaluated according to some algorithm, where e.g. the voltage is calculated first, and then the current. In Modelica, because it is a acausal modelling language, it is enough to simply declare the governing equations [15].

To be able to actually solve the system of equations formulated in the model in a numerical solver, it needs to be converted to a state space equation system. This involves determining a set of state variables, expressing their time derivatives as functions of state variables and input variables, and determining output variables as functions in terms of state variables and input variables. This is done automatically by the Modelica compiler, meaning that the model developer only needs to choose whatever variables that are most convenient, declare the basic equations in some preferred form, and leave it up to the compiler to derive the state space

equation system [15]. That the model in the present work is separated into convenient subcomponents does not influence how the equations are solved, because all the equations are solved simultaneously.

In thermodynamic systems, the Modelica compiler will typically select temperature and pressure as state variables for non-mixtures, and temperature, pressure and mass fraction for mixtures. A practical implication of this is that even though the accumulation term

$$\frac{\mathrm{d}}{\mathrm{d}t}\left(V \cdot \rho_{\mathrm{out}} \cdot u_{\mathrm{out}}\right)$$

in the heat balance (Eq. (3.1)) is given in terms of the specific internal energy u and density ρ, it will typically be manipulated at compilation time by the simulation engine to an expression in terms of the state variables pressure and temperature. Sometimes the choice of state variables varies, and the simulation engine may dynamically change state variables during simulation.

3.5.2 Boundary Values, Model Outputs and Solver

Referring to Fig. 3.1 there are four boundaries in the model; flue gas going into the water wall and out of the economizer and water going into the economizer and out of the final superheater. Both of the outlets are calculated in the model, and the two inlet boundaries of flue gas and water respectively needs to be defined by the user.

Mass fractions, temperature, pressure and mass flow rate are defined for the flue gas going into the water wall. It is assumed that complete combustion without heat losses occurs and thus the adiabatic combustion temperature should be used for the inflowing flue gas. The pressure is the atmospheric pressure, and the mass flow depends on the load.

For water going into the economizer, temperature, pressure and mass flow rate are defined, the latter two of them depending on the load.

The solution in Dymola, which is obtained with the dynamic time-stepping DASSL solver, includes many different outputs. Some examples are the total heat transfer in each component, all the thermodynamic state properties, and for some also their time derivatives, in the inlets and outlets of the components.

4

Results and Discussion

In this chapter the results of the thesis are presented. A fictional boiler is dimensioned for simulations to study the dynamic behaviour. Parameters such as the number of tubes and their dimensions, heat transfer areas, mass flows, and pressures are loosely based on values found in literature. The full load operating conditions of the boiler can be found in Tab. 4.1.

Table 4.1: Boiler operating conditions at full load

Parameter	**Value**
Thermal power	1055 MW
Live steam condition	300 bar/600°C
Water mass flow	445 kg/s
Flue gas flow	500 kg/s

Some of the boiler input parameters, as well as the model output temperatures and overall heat transfer coefficients at full load, are shown in Tab. 4.2. The total effective emissivity is 0.45 in both the water wall and the final superheater, which is a common value for coal combustion flue gas [10].

At both inlet boundaries, temperatures and mass flow rates are specified, the former are constant and the latter depending on the load. The economizer inlet temperature is constant at 250°C. The flue gas inlet temperature is 2200°C, which is a typical adiabatic combustion temperature for coal, and the composition is 75 % N_2, 17 % CO_2, 4 % H_2O, 4 % O_2. The pressure is specified at the inlet boundaries. It is the ambient atmospheric pressure for the flue gas and load dependent for the water.

Table 4.2: Component output values at full load and input parameters.

	Outputs			**Input parameters**		
	T_w [°C]		U	Area	Flue gas	Water
	Inlet	Outlet	[W/m^{2}K]	[m^2]	volume [m^3]	volume [m^3]
Economizer	250	370	80[1]	5 200	250	50
Water wall	370	510	—	1 480	3 800	115
Primary superheater	505	550	98[1]	1 350	500	20
Final superheater	550	600	—	640	500	20

The basis for evaluation of the boiler dynamic and steady-state behaviour is sliding pressure operation. Recall from chapter 2.2 that the flow and pressure of water defines the load, i.e. 90% load means 90% of the full load mass flow and pressure. Henceforth a load change refers to a change in economizer inlet pressure and flow. Only supercritical pressures are considered, thus limiting the minimum load to around 75% which corresponds to 225 bar.

4.1 Reference Scenario

As mentioned in chapter 2.2, load changes of 4-6 % of maximum rated power output per minute are possible, which serves a guideline for simulations. To emulate a load change, the water flow and pressure were ramped down by 5 % over a 60 second period a number of repeated times, separated by 1000 seconds to allow the boiler to reach steady-state in between. The flue gas flow was also decreased by 5 % over a 60 second period. At first, only the load range 100 %-75 % is considered, and the inlet property variations are shown in Fig. 4.1. The pressure ramp down in Fig. 4.1 is slightly smoothed out compared to the other two properties, this is due to a numerical stability problem that arises with the sharp derivatives at the "edges" of the ramps. This issue is discussed further in section 4.1.1.

The boiler response to the load changes is seen in Fig 4.2, which will henceforth be referred to as the reference scenario. There are several things noticeable with the results shown in Fig. 4.2. First of all, the steady-state temperatures drifts upwards with reduced load in Fig. 4.2(b) for all components except for the economizer. This is because the flue gas supplies more heat than what is required. Because the live steam condition is fixed at a certain load, the flue gas flow needs to be adjusted. The flue gas flow step reductions were consequently adjusted, while other parameters held constant, so that the steady-state live steam temperature stay at around 600°C. The result of the flow adjustment is seen in Fig. 4.3.

[1]The parameters to Eq. (2.18) are $S_T = 0.1\,\text{m}$, $N = 200$, $L = 10\,\text{m}$, $D = 0.08\,\text{m}$

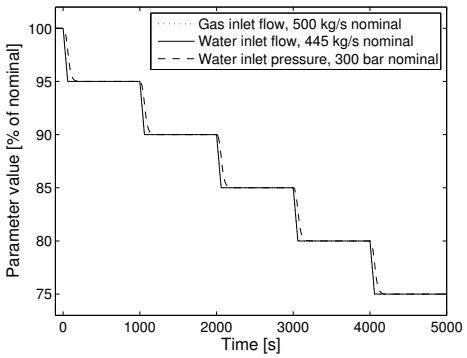

Figure 4.1: A series of decreases in flue gas and water inlet flow, and water pressure. The flue gas and water flow lines are overlapping in the figure.

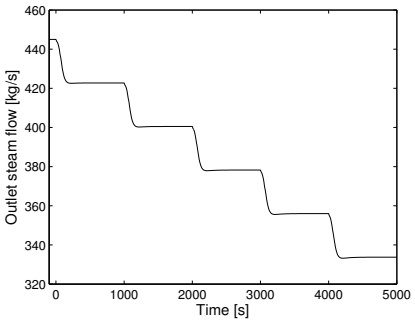

(a) Mass flow rate out of the final superheater.

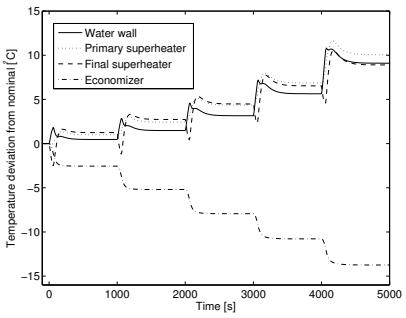

(b) Water outlet temperature deviation.

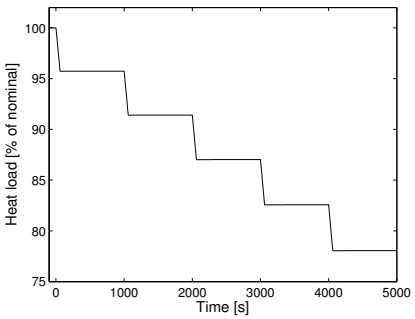

(c) Total heat transfer in the boiler. The nominal heat load is 1055 MW.

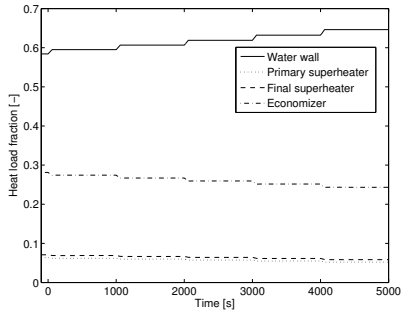

(d) Fraction of total heat transfer in the components.

Figure 4.2: Boiler outputs during a series of 5 % load changes taking place every thousand second, starting at $t = 0$ (see Fig. 4.1).

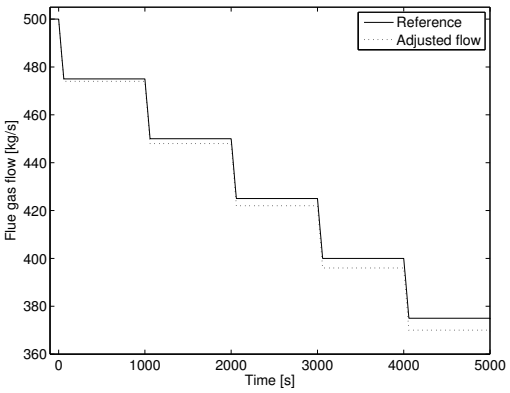

(a) Inlet flue gas flow before and after adjustment.

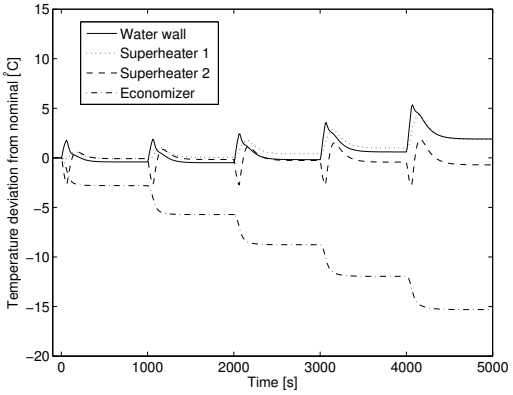

(b) Water outlet temperature deviation after adjustment.

Figure 4.3: Boiler output where flue gas flow is adjusted to maintain a steady-state live steam temperature roughly around 600°C.

The flue gas temperatures in the reference scenario can be seen in Fig. 4.4. The temperature is decreasing with each load reduction because the fraction of heat transfer in the water wall increases with decreasing load, see Fig. 4.2(d). The flue gas temperatures follow the changes in load without exhibiting any dynamic behaviour similar to the temperature swings seen on the water side in Fig. 4.2(b). The characteristics of the flue gas temperature was found to be similar in every investigated scenario and will thus not be discussed further.

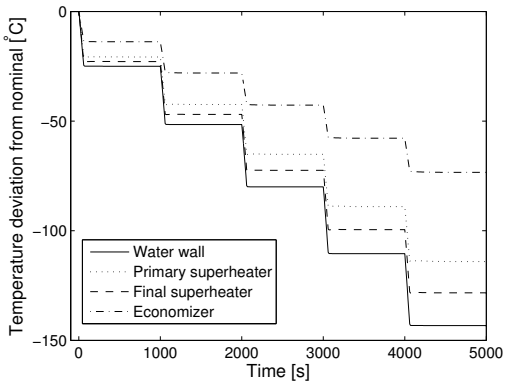

Figure 4.4: Flue gas temperature out of the components during the reference scenario. Nominal temperatures: 1287°C, 1171°C, 1070°C, 586°C out of the water wall, final superheater, primary superheater and economizer respectively. The water wall inlet temperature is constant at 2200°C.

Comparing Fig. 4.2(b) to Fig. 4.3(b), the dynamic response on the water side shows the same characteristics and thus the following reasoning is valid for both cases. First of all, the time it takes to reach new steady-state conditions is fairly short. The temperatures takes around 500 seconds and the flow of water out of the components around 200 seconds to stabilise at new values, the latter is illustrated in Fig. 4.5. There is in principle no delay in the outlet flow of the economizer compared to its inlet flow.

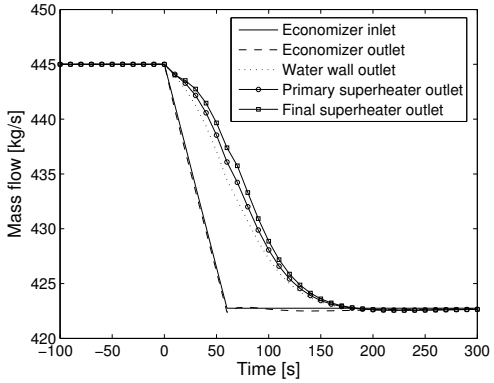

Figure 4.5: Flow of water out of each component during the first load decrease, compared with the inlet flow to the economizer.

4.1.1 Transient Water Temperatures

The dynamic temperature behaviour in the reference scenario is similar in all step reductions. Figure 4.6 shows the water temperatures during the first load change.

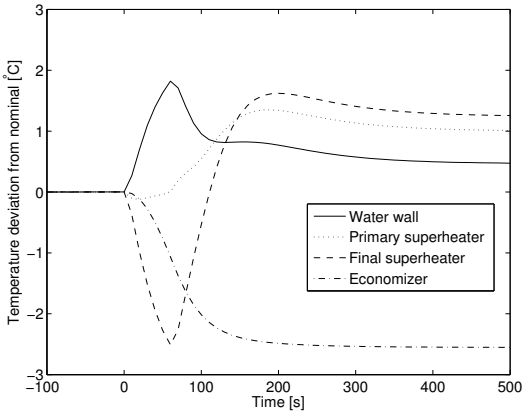

Figure 4.6: Water outlet temperatures during the first load in the reference scenario.

Because of the assumptions in the model, anytime the pressure changes in the inlet, the change travels instantaneously throughout the system, while the mass flows and temperatures take some time to adjust to a load change. This might be the reason for the temperature drop seen for the primary and final superheater temperatures in Fig. 4.6. While the pressure changes instantaneously, it takes some time for the flow reduction to travel throughout the system as illustrated in Fig. 4.5. Looking at the mass balance, Eq. (3.2), from $t = 0$ and a short period thereafter

$$\frac{\mathrm{d}}{\mathrm{d}t}(V\rho_{\mathrm{out}}) = \dot{m}_{\mathrm{in}} - \dot{m}_{\mathrm{out}} \approx 0,$$

which is saying that there is a constant mass of steam enclosed in the superheater. A fixed mass of steam that expands due to a pressure reduction will drop in temperature, which is what happens here. However, soon the mass flow reduction reaches the superheater and the temperature increases again.

As mentioned, the pressure ramp downs are smoothed out slightly compared to the water and flue gas flow ramp downs. No converged solutions were obtained when removing this smoothing, and the cause is likely that the above pressure effect becomes stronger with a larger pressure derivative.

The effect seen in the final superheater is also found in the primary superheater, but the extent of the temperature drop is less. This is consistent with the fact that the flow reduction reaches the primary superheater earlier, thus reducing the effect.

In the water wall, there is instead a temperature increase. Looking at Fig. 4.5, it can be seen that there is in principle no lag in the outlet flow of the economizer, and thus no lag in the inlet flow of the water wall. Looking at the mass balance for the water wall, from $t = 0$ and a short period thereafter

$$\frac{\mathrm{d}}{\mathrm{d}t}(V\rho_{\mathrm{out}}) = \dot{m}_{\mathrm{in}} - \dot{m}_{\mathrm{out}} < 0.$$

There is thus effectively less mass of water to heat up in the water wall, which explains the temperature increase. The above pressure effect should be present in the water wall as well and can be expected to have a dampening effect on the temperature increase.

Steam is to some extent compressible, meaning that a pressure change does not travel instantaneously in a real boiler. This was incorporated into the simulations as a delay of the pressure decreases by 10 seconds relative to the other ramp downs. As can be seen in Fig. 4.7, which shows the first load change, the temperature response is quite different. The temperature drop in the final superheater is smaller because the flow changes have had time to propagate before the pressure is reduced. In the primary superheater there is now a temperature increase instead of a decrease. The temperature increase in the water wall is larger, which is consistent with the dampening effect of the pressure reduction discussed above now being delayed.

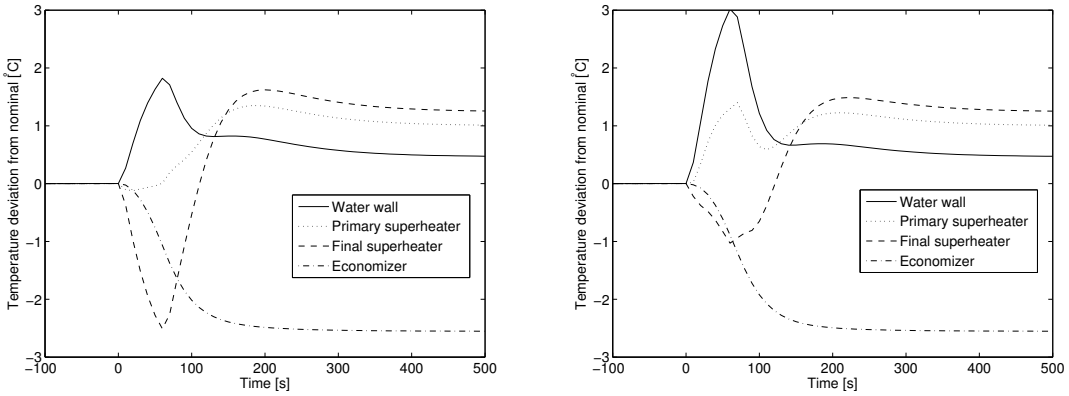

(a) Reference scenario.

(b) Pressure decreases delayed 10 seconds.

Figure 4.7: Water outlet temperature deviation, reference scenario in (a) and delayed pressure reduction in (b) during the first load change.

4.2 Scenario Variations

Here some variations to the reference scenario are carried out to see the effect on the dynamic behaviour.

4.2.1 Influence of Step Size

Slowing down the ramp downs in the reference scenario, from 60 seconds to 120 seconds, gives the same characteristics in the temperature response. Comparing the reference scenario in Fig. 4.8(a) with the slower ramp scenario in Fig. 4.8(b), it can be seen that the amplitude of the dynamic temperature deviations are somewhat less.

The characteristics are the same when increasing the step size, from 5% to 12.5%, over the same 60 second time span. Figure 4.9 shows the temperature response for the larger step sizes compared to the reference scenario from 100 % to 75 % load. The total simulation time in the larger step size scenario is 2000 seconds because only two step reductions are necessary. It can be noted that the temperature swings become more severe.

4.2.2 Load Increases

The boiler response is reversed when running the reference scenario backwards, i.e. a series of load increases according to Fig. 4.10(a). The temperatures can be seen in Fig. 4.10(b) and now instead there is a temperature increase in the superheaters and a temperature drop in the water wall. It can also be noted that the amplitude of the swings are somewhat larger than in the reference scenario.

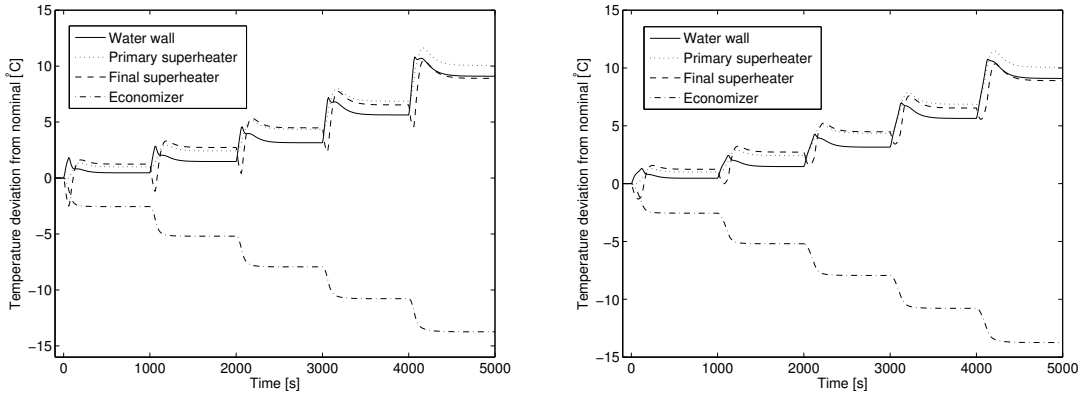

(a) Reference scenario. **(b)** Slower ramp downs.

Figure 4.8: Water outlet temperature deviation. Reference scenario in (a) and slower ramp downs in (b).

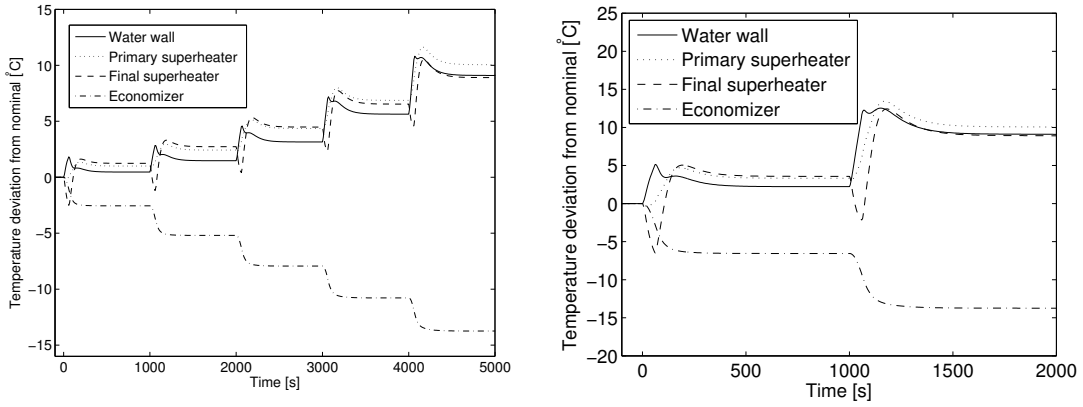

(a) Reference scenario. **(b)** Larger step size.

Figure 4.9: Water outlet temperature deviation. Reference scenario in (a) and larger step size in (b).

4.2.3 Influence of Water Volume Parameter

The volumes in each of the components are input parameters (see Tab. 4.2). To see the effect of changing these parameters, the reference scenario was simulated with the water volumes halved respectively doubled. The result is presented in Fig. 4.11. Halving the water volumes means that the system reacts quicker to the change in flow, so quick in fact in this case that a temperature peak is seen in all components except for the economizer. Less water in each volume also means less inertia, which explains why the temperature peak in the water wall is stronger.

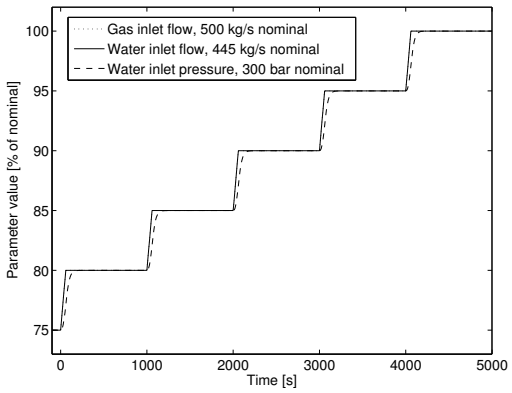

(a) Inlet boundary input values from 75% to 100% load. The flue gas and water flow lines are overlapping in the figure.

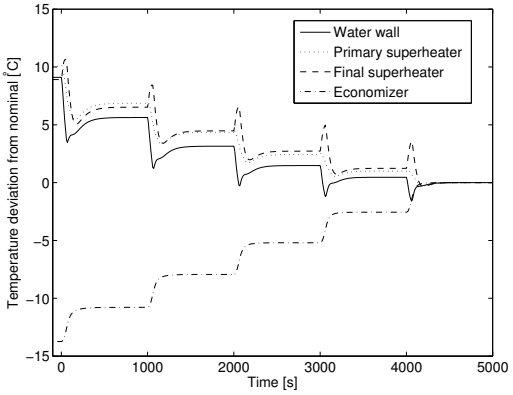

(b) Water outlet temperature deviation.

Figure 4.10: Reference scenario in reverse, i.e. a series of load increases from 75% to 100% load, starting at $t = 0$.

Doubling the water volume has a reversed effect, i.e. it takes longer to adjust to the new flow. The temperature decreasing effect of the pressure reduction becomes more important and leads to the increased temperature drop in the superheaters and a lessened temperature increase in the water wall.

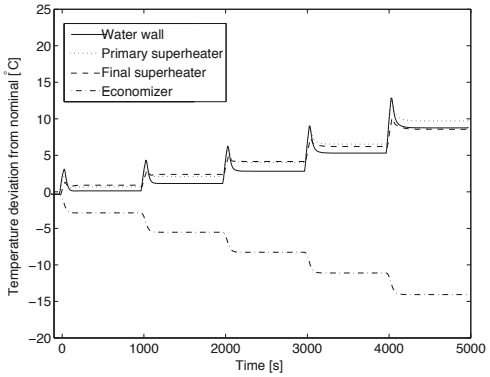

(a) Halved volume.

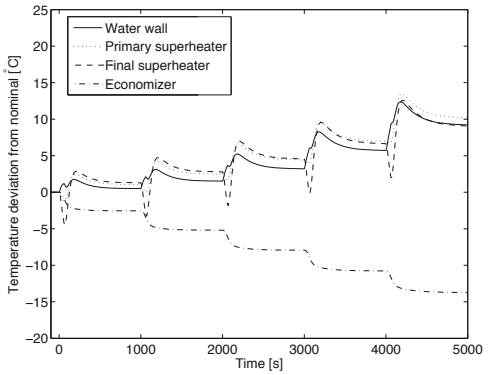

(b) Doubled volume.

Figure 4.11: Water outlet temperature deviation.

4.2.4 Desuperheating

A desuperheater was inserted after the final superheater to see if it can reduce the temperature drift seen in Fig. 4.2(b). Water at the same pressure and temperature as what is going into the economizer was used as cooling stream. The temperature before and after the desuperheater for the reference scenario can be seen in Fig. 4.12 which clearly shows that the temperature is rapidly reduced and maintained around 600°C. Only a small flow of cooling water is required, peaking at around 2 kg/s.

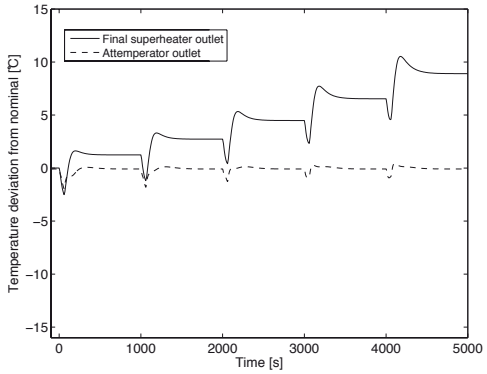

Figure 4.12: Temperature before and after the desuperheater during the reference scenario.

5

Conclusions and Discussion

In accordance with the aim, a dynamic model of the heat and mass transfer in a supercritical once-through boiler have been developed. The model is highly flexible in its implementation, and the modular design makes it easy to adapt it to resemble actual boiler designs. Inserting it into a complete steam cycle should be fairly unproblematic since the model was developed using the in-house standards that are the practice at Solvina. Without having access to experimental data or knowledge of how a real boiler responds to transient events, the extent to which the present model reflects a real boiler needs to be investigated further.

The simulation results indicate that the water temperature response during load changes is governed mainly by flow dynamic phenomena that arises due to rapidly changing pressure and flow. The heat transfer, as it is modelled here, seem to not have a large influence on the dynamic behaviour.

The presented model, that uses a low number of discretizations and lumped variables in large volumes, can intrinsically not capture local transient events that may be important in real boiler operation. For example, local heat flux distribution deviations is something that the plant operator may be interested in but is not something that a model of this type can capture.

Having in mind that the purpose of the present boiler model as a piece in a power plant simulator, it can be argued that the level of detail is sufficient. The focus in a plant operator simulator lies very much in the dynamics of the control system and how it acts during different events, and for this purpose it is enough if the boiler model captures the general large scale dynamic behaviour.

6

Future Work

The presented model should be seen as a framework to be extended upon, and the results presented highlights a number of issues that should be addressed in further development. First of all, the presented results show that how the pressure is varied greatly influences the dynamic response. Therefore one should consider including the pressure dynamics.

Only supercritical pressures have been considered, but sliding pressure once-through boilers operate at subcritical pressure when the load is low. Subcritical pressure leads to two-phase flow in the water wall, and the heat transfer model presented may not be representative for such conditions.

The thermal inertia of the tube material can be expected to have an impact on the dynamic behaviour of the boiler. Knowing the tube mass and heat capacity it is an easy task to include the inertia effect in the model, e.g.

$$\frac{\mathrm{d}}{\mathrm{d}t}(\mathrm{Cp}_s m_s T_s) = \dot{Q}_g - \dot{Q}_w$$

The firing systems are quite elaborate in e.g. a pulverised coal boiler, and one must consider the dynamics of the coal mills, the fuel feeding system and the combustion air intake, which are all important factors for the control system. Due to the adaptability of the boiler model, this would simply be a matter of connecting the flue gas inlet boundary of the boiler to some sort of combustion model. Something to consider is that actual boiler configurations utilise staged combustion, with several levels of burners extending some vertical distance in the furnace and thus it may be necessary to divide the water wall model into several sections for a more accurate representation.

Since the radiation governs the majority of the heat transfer, it is reasonable to expect that it greatly influences the dynamic behaviour of the boiler. Some of

this dynamic is lost when using a simplified radiation equation such as the one used here. The effective emissivity is assumed to be constant, i.e. assuming that particulate and gas emissivity as well as the flame properties are constant while they are likely load dependent in reality. Therefore it may be advisable to include a more elaborate model of the emissivity for better accuracy.

Bibliography

[1] Energy Technology Perspectives 2008, International Energy Agency, 2008, p. 257.
URL http://www.iea.org/textbase/nppdf/free/2008/etp2008.pdf

[2] P. Weitzel, Steam Generator for Advanced Ultra-Supercritical Power Plants 700 to 760C, Babcock & Wilcox Power Generation Group, 2011.
URL http://www.babcock.com/library/pdf/br-1852.pdf

[3] A. Rovira, M. Valdes, M. D. Duran, A model to predict the behaviour at part load operation of once-through heat recovery steam generators working with water at supercritical pressure, Applied Thermal Engineering 30 (13) (2010) 1652 – 1658.

[4] The IAPWS Industrial Formulation 1997 for the Thermodynamic Properties of Water and Steam, Journal of Engineering for Gas Turbines and Power 122 (1) (2000) 150–184.

[5] V. Grabezhnaya, P. Kirillov, Heat transfer under supercritical pressures and heat transfer deterioration boundaries, Thermal Engineering 53 (2006) 296–301.

[6] J. H. Potter, The joule-thomson effect in superheated steam, Journal of Engineering for Industry 92 (2) (1970) 257–262.

[7] Siemens Power Generation, Benson boilers for maximum cost-effectiveness in power plants (2001).
URL http://www.energy.siemens.com/us/pool/hq/power-generation/power-plants/steam-power-plant-solutions/benson%20boiler/BENSON_Boilers_for_Maximum_Cost_Effectiveness.pdf

[8] B. P. Vitalis, Constant and sliding-pressure options for new supercritical plants, Power.

URL `http://www.powermag.com/coal/Constant-and-sliding-pressure-options-for-new-supercritical-plants_491.html`

[9] N. Lallemant, A. Sayre, R. Weber, Evaluation of emissivity correlations for H_2O-CO_2-N_2/air mixtures and coupling with solution methods of the radiative transfer equation, Prog. Energy Combustion Science 22 (6) (1996) 543–574.

[10] K. Strauss, Kraftwerkstechnik: Zur Nutzung Fossiler, Nuklearer Und Regenerativer Energiequellen, Vdi-buch, Springer, 2009.

[11] M.-N. Dumont, G. Heyen, Mathematical modelling and design of an advanced once-through heat recovery steam generator, Computers & Chemical Engineering 28 (5) (2004) 651–660.

[12] Heat Transfer Equipment Design and Performance, CRC Press, 2002.

[13] J. R. Welty, C. E. Wicks, R. E. Wilson, G. L. Rorrer, Fundamentals of Momentum, Heat and Mass Transfer, John Wiley & Sons, 2008.

[14] S. E. Mattsson, On modeling of heat exchangers in modelica, in: Proceedings of the 9th European Simulation Symposium, 1997.

[15] Modelica - A Unified Object-Oriented Language for Physical Systems Modeling - Language specification version 3.1, Modelica Association, 2009.
URL `https://www.modelica.org/documents/`